frontiers in Materials

ORIGINAL RESEARCH
published: 20 March 2020
doi: 10.3389/fmats.2020.00053

A Study on the Electric Surface Potential and Hydrophobicity of Quartz Particles in the Presence of Hexyl Amine Cellulose Nanocrystals and Their Correlation to Flotation

Robert Hartmann and Rodrigo Serna-Guerrero**

Department of Chemical and Metallurgical Engineering, School of Chemical Engineering, Aalto University, Aalto, Finland

OPEN ACCESS

Edited by:
Jan Zawala,
Institute of Catalysis and Surface Chemistry (PAN), Poland

Reviewed by:
Onur Guven,
Adana Science and Technology University, Turkey
Way Foong Lim,
University of Science Malaysia, Malaysia

****Correspondence:***
Robert Hartmann
robert.hartmann@aalto.fi
Rodrigo Serna-Guerrero
rodrigo.serna@aalto.fi

Specialty section:
This article was submitted to Colloidal Materials and Interfaces, a section of the journal Frontiers in Materials

Received: *29 November 2019*
Accepted: *18 February 2020*
Published: *20 March 2020*

Citation:
Hartmann R and Serna-Guerrero R (2020) A Study on the Electric Surface Potential and Hydrophobicity of Quartz Particles in the Presence of Hexyl Amine Cellulose Nanocrystals and Their Correlation to Flotation. Front. Mater. 7:53. doi: 10.3389/fmats.2020.00053

In this work, the study of hexyl amine cellulose nanocrystal (HAC) as a renewable and environmentally-friendly reagent for the flotation of quartz (QRZ) is expanded with a focus on the changes of electrical states at the solid-liquid interface, the range of solid-gas interactions, and their impact on flotation operations under a turbulent regime. Furthermore, particle-bubble attachment probabilities were measured with the recently engineered automated contact timer apparatus (ACTA), a versatile technique used to deduce the wettability of microparticles and potentially predict their floatability. Therefore, the findings of the ACTA proved that, with sufficiently hydrophobic QRZ (i.e., HAC concentration $\geq$ 0.667 $mg_{HAC}/m^2{}_{QRZ}$), stable particle-bubble attachments occur at particle-bubble distances in the range of tens of micrometers. The distances for the successful attachment of HAC-coated QRZ particles exceed the range of interactions reported in literature so far and imply the existence of structural or hydrodynamic phenomena acting between particle and bubble surfaces. The occurrence of so-called non-compressive particle-bubble attachments is shown to correlate with a significant increase in the floatability of QRZ, where recoveries up to 90% were obtained. Based on the experimental results, some insights on the nature of the long-range interactions responsible for the particle-bubble attachment of hydrophobic particles are provided.

Keywords: cellulose-derived reagent, surface (zeta-) potential, hydrophobicity, particle-bubble-attachment, induction timer, floatability

INTRODUCTION

Froth flotation is a widely used industrial process for the concentration of mineral particles. Despite its widespread application in the field of mineral processing, the process performance has not changed significantly during the last decades and the understanding of phenomena responsible of flotation is still strongly based on empirical knowledge. Nowadays, this traditional approach is

challenged by the demand to process ores with decreasing grades (Calvo et al., 2016) and thus, many efforts have been recently undertaken to better understand the various aspects of flotation processes with the aim of enhancing their efficiency. Simultaneously, the growing concerns in terms of environmental impact and consumption of natural resources urge for the design of mineral flotation processes with minimal impact, including for example, efficient water recycling strategies and the employment of more environmentally-friendly chemicals (Bridge, 2004; Pearse, 2005; Liu et al., 2013; Nuorivaara et al., 2019).

To that end, chemicals derived from renewable sources, for instance cellulose, hemicellulose or lignin, are promising substitutes to the State-of-the-Art reagents in various fields, although their use in the mineral processing industry remains largely unexplored (Klemm et al., 2005; Ago et al., 2016). In terms of flotation, the relatively high chemical complexity of functionalized nanocellulose leads, on one hand, to challenges concerning their surface interaction mechanisms, but on the other hand, to opportunities to modify macromolecules with tailored properties that selectively interact with specific mineral species rendering them more hydrophobic. So far, cellulose-based chemicals (e.g., starch dextrin, guar gum, carboxymethyl cellulose or chitosan) have proven useful as depressants (Mu et al., 2016; Hernandez et al., 2017). In addition, research was recently initiated to investigate the efficiency of artificial nanoparticles as collectors, however, the behavior of nanoparticles differs significantly from conventionally used soluble organic molecules (Yang et al., 2011; Yang et al., 2013; Dong et al., 2017; Abarca et al., 2018). In a study of Abarca et al. (2018), polystyrene nanoparticles were modified by click chemistry to incorporate several functional groups on the nanoparticles surface. In such work, tests were performed to study colloidal stability and hydrophobicity, leading to flotation recoveries up to 90% for the most suitable candidates. The employment of nanoparticles as collector in froth flotation introduces novel aspects of study, such as the colloidal stability of the hydrophobic nanoparticles in the pulp or the occurrence of "wet-patch" adhesions, in which only the adsorbed hydrophobic nanoparticles attach to an air bubble, while the mineral particles remains completely wetted by water (Yang et al., 2011). So far, most of the work with nanoparticles was performed with artificial polymers, which are not biodegradable and their synthesis is rather complicated (Al-Shatty et al., 2017). In this study, hexyl amine cellulose nanocrystal (HAC) was used as an alternative of commercial amine-based collectors or artificial nanoparticles for quartz (QRZ) flotation. To our best knowledge, aminated celllose nanocrystals are the first bio-based nanoparticle used as collector in froth flotation (Laitinen et al., 2016; Hartmann et al., 2017, 2018).

The behavior of different aminated cellulose nanocrystals dispersed in an aqueous solution, as well as the change of the wetting properties of quartz surfaces after its adsorption, was part of previous studies by the authors (Hartmann et al., 2016, 2017, 2018; Lopéz et al., 2019). In such studies, the influence of nanocellulose on the surface charge of QRZ was identified using zeta potential and it was correlated with the floatability of QRZ using a single-bubble Hallimond tube. While such studies showed promising results, it was also found that the performance of HAC as collector differs fundamentally from conventional reagents, due to its greater spatial dimensions, the water-insoluble nature of HAC nanoparticles, and its complex chemical constitution. Indeed, the origin of the pulp and the modification route of HAC may have an effect on its chemical constitution. In case of HAC, amine groups can be incorporated into the cellulose structure in a way that the nitrogen atom forms a covalent bond with an oxygen atom of the cellulose backbone, while its hydrocarbon chain is oriented toward the exterior. Therefore, the amine functional groups in HAC can be considered different from amine functionalities in conventional amphiphilic water-soluble molecules, where the nitrogen atom is only bound to a carbon atom of its linked hydrocarbon chain. It has been shown that the aqueous environment affects the protonation of the amine groups in HAC and their reactivity (Hartmann et al., 2016). Another fundamental difference to conventional reagents is the random distribution of functional groups throughout the entire structure of HAC. Consequently, the amine groups relevant for interactions with surrounding phases are rather isomorphically distributed than positioned toward a single direction. Interestingly, the degree of protonation of the amine groups has positive effects on its adsorption on QRZ, but may have antagonistic effects on the rupture of the liquid intervening film between a particle and a bubble (Hartmann et al., 2018). For these reasons, it is worth to continue exploring the behavior of HAC in the mineral processing field.

To characterize the efficiency of flotation processes, efforts have been placed to define physico-chemical parameters, which could be capable to reliably predict the floatability of a mineral species without expensive experimental schemes. The use of three-phase contact angle, for example, has proven unreliable due to the difficulties of measuring contact angles of microparticles or on rough surfaces (Crawford and Ralston, 1988). Recently, the use of thermodynamic properties of minerals were investigated, such as the free energy of interaction between a particle and a bubble immersed in water (ΔG_{pwb}) (Hartmann et al., 2017; Rudolph and Hartmann, 2017) or the enthalpy of immersion (ΔH_{imm}) (Taguta et al., 2018, 2019). These parameters allow a more precise determination of the energetic state of a mineral surface, but their measuring techniques are limited. For example, there is no aqueous phase during measurements in case of the inverse gas chromatography (Hartmann et al., 2017; Rudolph and Hartmann, 2017), and particles with sizes significantly finer as the ones processed in real flotation practice are required in case of calorimetric measurements (Taguta et al., 2018, 2019). In addition, these techniques measure properties at equilibrium states instead of dynamic systems.

Another approach to predict floatability of a particular mineral system is the study of induction time, defined as the time required to drain the intervening liquid film between a particle and a bubble leading to the formation of a stable, orthokinetic three-phase contact. In a review published by Verrelli and Albijanic (2015), the strengths and weaknesses of several methods to measure the induction time were summarized. To overcome the current limitations of the previously available experimental methods, a novel automated contact timer apparatus (ACTA) was engineered by our research group (Aspiala et al., 2018).

This apparatus offers various technical advantages, such as a controlled preparation of a particle bed, the ability of setting and recording contact times, approach and receding speeds, and the measurement of hundreds of individual attachment events in a few hours. In addition, the ACTA allows the possibility to mimic environments present in flotation cells and the use of particles with relevant sizes. Most importantly, the ACTA is capable of analyzing both, the time and distance at which a particle-bubble attachment occurs with a certain probability. The establishment of particle-bubble attachment probability distributions as a function of contact time and distance may be the key to characterize the degree of hydrophobization of a particulate sample and predict its floatability. In a recent work by the authors, it was found that, with sufficiently hydrophobic particles, a stable particle-bubble attachment occurs even at distances of tens of micrometers (Hartmann and Serna-Guerrero, 2020). This has a tremendous effect on the understanding of particle-bubble attachments, further demonstrating that hydrophobic forces may lead to capillary forces that have a further reach than the interactions derived for instance from surface force apparatus or atomic force microscopy using the extended DLVO theory, which are generally accepted to act within distances in the nanometer-range (Derjaguin and Churaev, 1989; William et al., 1994; Yoon and Moa, 1996; van Oss, 2003).

The present work thus combines a series of experimental studies to determine the changes at the surface level of QRZ in the presence of HAC and its influence on the particle-bubble attachment. Firstly, the evolution of the electrical state of QRZ particles in the presence of different HAC concentrations and environments is analyzed. Subsequently, the probability of particle-bubble attachments dependent on the contact time and particle-bubble distance is analyzed using the above-described ACTA. As will be discussed, non-compressive particle-bubble attachments were observed at distances beyond the limits of measurable effects of interaction energies known in literature and may hold the key for an objective assessment of floatability using attachment probabilities. To demonstrate the practical applicability and hydrophobic nature of HAC, bench-scale flotation tests were performed, showing that HAC is an efficient collector for QRZ. Furthermore, this study shows for the first time a correlation between high QRZ recoveries and the presence of non-compressive attachments between particles and bubbles in ACTA measurements.

MATERIALS, METHODS, AND MODELS

Quartz and Aminated Cellulose Nanocrystals

Quartz (QRZ) was supplied by Nilsiä (Sibelco, Nilsiä, Finland, 99.2% purity, 100–600 μm) and ground in a mill (Fritsch *PULVERISETTE*, planetary micro mill) for 15 s. The ground QRZ powder was dry sieved (Fritsch *ANALYSETTE*, vibratory sieve shaker) between sieves with 75 and 180 μm mesh-opening sizes. Afterward, the QRZ fraction was immersed in de-mineralized water, treated for 3 min with ultrasound (Branson 5510 Ultrasonic Cleaner) at 40 kHz, placed on a 75 μm mesh size sieve and washed with de-mineralized water to remove fines. The wet-sieved material was collected and dried in an oven overnight at 50°C. The sample thus obtained was used for the ACTA and flotation experiments. For the electrophoretic mobility analysis, a sample of a fine quartz powder was prepared as previously described (Hartmann et al., 2018). The granulometric properties of the fine and coarse quartz fractions are summarized in **Table 1**, based on laser diffraction (Beckman Coulter LS 320) and nitrogen adsorption (ASAP 2020 N_2, micromeritics) following the Brunauer-Emmet-Teller method.

As collector reagent, hexyl-amine cellulose nanocrystals (HAC) were synthesized according to the procedure of Visanko (Visanko et al., 2014; Hartmann et al., 2016). Using this method, a suspension of 0.1-wt% HAC was obtained with nanocrystals possessing a length of 137 nm ± 6 nm and diameter of 5 nm ± 0.2 nm (Hartmann et al., 2018).

The Electric Surface Potentials From Electrophoresis

The electrophoretic mobility of QRZ in the presence of HAC with different concentrations, background salts and pH values was measured with a Delsa Nano C zeta-potential analyzer (Beckman Coulter, United States). Prior to the experiments, different background salt solutions were prepared using de-mineralized water with controlled pH values of 5, 7, or 9 (Mettler Toledo Seven Excellence) obtained by the addition of diluted HCl or NaOH solutions. After the pH value remained constant for 24 h, background salts were added to obtain either a 10 mM NaCl solution or a 1 mM $MgSO_4$ solution. It was assumed that the addition of salts did not alter the initial pH value. For each experiment, 10 mg of quartz were dispersed in 30 ml of background salt solution and stirred for 5 min. Meanwhile, HAC was treated in an ultrasonic bath for 3 min. Subsequently, different amounts of HAC were added to the QRZ suspension to reach concentrations of 0.5, 1, 1.5, 2, 2.5, or 3 mg/l. The suspension thus obtained was stirred for one additional minute to promote HAC adsorption on QRZ. After stirring, the suspension stood still for 2 min for coarse particles or flocculates to settle and then approximately 3 ml of the

TABLE 1 | Size quantiles and specific surface areas and Sauter diameters ($D_{3,2}$) of quartz fractions based on particle size distributions obtained through laser diffraction and the Brunauer-Emmet-Teller method.

Granulometric properties	Quartz	
	Fine (electrophorese)[a]	Coarse (ACTA/flotation)
D_{10}/μm	1.3	94
D_{50}/μm	6.1	154
D_{90}/μm	21.2	249
$D_{3,2}$/μm	1.3	151
$S_{spec,calc}/m^2g^{-1}$[b]	0.772	0.015
$S_{spec,BET}/m^2g^{-1}$	1.7009	0.045

[a]*From Hartmann et al. (2018).* [b]*Specific surface area calculated from laser diffraction results.*

suspension were transferred into the Delsa Nano C analyzer. During the measurement, the temperature was kept constant at 25°C and three measurements were performed on each sample for reproducibility. For each HAC concentration, measurements were performed on duplicates. For the determination of the electric surface (ζ−) potential, the Einstein-Smoluchowski equation was applied (Zembala, 2004).

$$\zeta = \frac{\eta \cdot u_{el.-phor.}}{\varepsilon_0 \cdot \varepsilon_{rel}} \quad (1)$$

where η is the dynamic viscosity of water at 25°C, $u_{el.-phor.}$ the detected electrophoretic mobility, ε_0 the permittivity of a vacuum and ε_{rel} the relative permittivity of water.

The Automated Contact Time Apparatus (ACTA)

For measurements with the ACTA, identical background salt solutions as previously described were used. For conditioning, 10 g of QRZ were transferred into a glass beaker containing 100 ml of background salt solution and stirred for 5 min. Meanwhile, a suspension of HAC was treated for 3 min with ultrasound. Afterward, the HAC suspension was mixed with the QRZ-containing suspension and the conditioning continued under stirring for 5 min. The concentrations of HAC in the suspension were set to either 3 or 5 mg/l. After conditioning, QRZ particles and background salt solution were transferred into a transparent plastic pool. The plastic pool was placed into the ACTA and a particle bed with a 2 mm thickness prepared by the automatically controlled shovel in the ACTA setup. Once a flat particle bed was obtained, the measurements were started. The contact times between bubbles and the particle bed were set at 20, 40, 60, 80, or 100 ms. The presence of an attached particle and the diameter of each bubble was recorded and measured using a microscopic camera positioned at the bottom of the pool (see **Figure 1**). The distance between needle tip and particle bed were measured with a high-speed camera positioned perpendicular to the movement of the needles to obtain the particle-bubble distance (see **Figure 1**). Each experiment consisted of 396 particle-bubble attachment events, which were individually analyzed on whether this resulted in a successful attachment, depending on the contact time and position. The operating principle of the ACTA measurement is visualized in **Figure 1** and a detailed description of the operation and data processing methodology can be found in Hartmann and Serna-Guerrero (2020). Since the previous work, the illumination of the bubbles during the recording with the high speed camera video has been improved, leading to a more accurate determination of the bubble-particle bed distance.

Flotation Tests

Bench-scale flotation tests were carried out in a 1.5 l Outokumpu flotation cell. A fresh background solution was prepared for each experiment with 10 mM NaCl or 1 mM $MgSO_4$. In addition, DowFroth 250 (DF250) at a concentration of 10 ppm was used as frother. The pH of the solution was controlled at either 5, 7, or 9. Approximately 300 g of QRZ were transferred into the flotation cell and the background salt solution added. The suspension was stirred for 5 min at 1300 rpm. At the same time, the HAC suspension was treated with ultrasound for 3 min. The rotational speed of the rotor was then reduced to 900 rpm and HAC suspension was added to the flotation cell for a concentration of either 3 or 5 mg/l and further conditioned for 5 min. Then, air was introduced at a flow of 4 l/min, at which point the flotation experiment was considered to have started. The total flotation time was 10 min and subsequently the over- and underflow were collected. In case of strong froth formation, additional background salt solution was added throughout the experiment to keep the water level constant. After each experiment, the over- and underflow was vacuum filtered and dried in an oven at 50°C, before their masses were measured. All experiments were performed as duplicates.

Overview of Examined Conditions for the Comparability of the Results

In the sections above, the concentration of HAC was presented as a relation of the dry mass of HAC to the volume of aqueous solution. However, to account for the different sizes and masses of the QRZ samples used in the various analysis methods described above, the results are presented as the relation of the mass of HAC in suspension to the free surface area of QRZ obtained with the BET method as an approximation for the fair comparison of the results. The HAC concentrations used in the different experiments of this work are summarized in **Table 2**. Please note that the values presented as $mg_{HAC}/m^2{}_{QRZ}$ may not necessarily represent the actual mass of HAC adsorbed on QRZ.

RESULTS AND DISCUSSION

Electrophoretic Mobility of Quartz Coated With Hexyl-Amine Cellulose

The importance of electric surface (ζ−) potentials on the physisorption of ionic molecular surfactants on QRZ and of the obtained particle-surfactant aggregate ζ-potential on their floatability is well accepted (Fuerstenau and Jia, 2004; Fuerstenau and Pradip, 2005). However, the replacement of conventional amphiphilic molecules by macromolecular HAC is not trivial. The presence of free surface charges on the HAC surface significantly affects both its adsorption on a mineral surface and the formation of a stable three-phase contact during flotation processes. This was presented and discussed in a previous work examining the selective flotation of QRZ from a mixture with hematite (Hartmann et al., 2018). The change of the derived ζ-potential of QRZ in the presence of different HAC concentrations is shown in **Figure 2**. For a better understanding, the results of the ζ-potentials of pure particles are shown from previous work (Hartmann et al., 2018) together with the results for a bubble dispersed in a 10 mM NaCl and 1 mM CaCl solution from Yang et al. (2001), assuming that Ca^{2+}- ions have a comparable behavior to Mg^{2+}- ions due to their physico-chemical similarity.

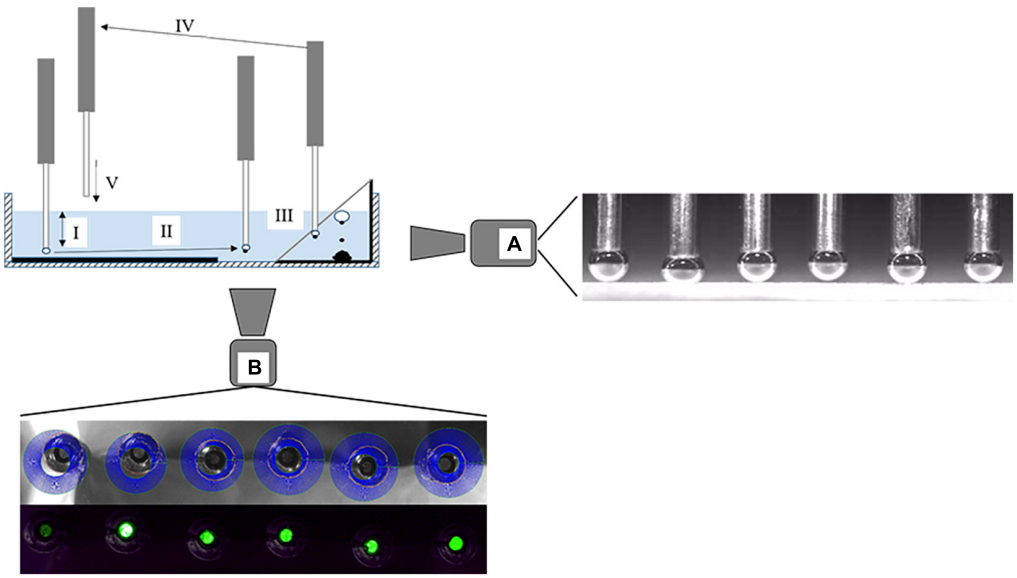

FIGURE 1 | Operating diagram of the ACTA with typical steps of a measurement cycle: (I) Bubbles are formed and approach the particle bed, rest for a set contact time and recede afterward again to the initial position. The initial distances of the needles varied to obtain different H between bubbles and the particle bed for a set contact time and the approach, rest and retraction of the bubbles are recorded with a high-speed camera (A). A representative image of the position of the bubbles relative to the particle bed at closest approach is given next to camera (A). (II) Bubbles are moved to the viewing window and images are taken by a digital microscope (B), representative images for the bubble size analysis and particle detection are shown below microscope (B). (III) Bubbles are moved to a collection bin and detached from the needles. (IV) The needles are lifted up until the needle tips are above the liquid, flushed with air for cleaning and simultaneously moved horizontally. (V) The needles are lowered slowly over an untouched spot of the particle bed into the liquid and the next cycle starts (as adapted from Hartmann and Serna-Guerrero, 2020).

The ζ-potential of pure substances shows that HAC possesses a positive ζ-potential for the examined pH range, approaching a neutral potential at pH 9, while QRZ is negatively charged, indicating a potential for attractive electrostatic interaction between them. By comparing the effect of the background solutions, the interactions between QRZ and polyvalent SO_4^{2-}- and Mg^{2+}- ions are stronger compared to monovalent Na^{+}- and Cl^{-}- ions, leading to a more pronounced compensation of its ζ-potential. For HAC, the reduction of the ζ-potential was only slightly stronger for the polyvalent background salts, taking in mind that the concentration of NaCl was ten times higher than of $MgSO_4$. Consequently, HAC is expected to physisorb on the mineral surface, which is proven by the two plots showing the distribution of the ζ-potential of QRZ for different HAC concentrations in the two salt solutions hereby studied. In general, all distributions show an evolution of the ζ-potential toward a maximum value with increasing HAC concentration. Eventually, the ζ-potential values reach a plateau, indicating the complete occupation of active sites at the QRZ surface. For QRZ and HAC dispersed in NaCl, HAC overcompensates the ζ-potential of QRZ in pH 5 and 7 with an isoelectric point at 0.4 $mg_{HAC}/m^2{}_{QRZ}$ and 1.4 $mg_{HAC}/m^2{}_{QRZ}$, respectively. At pH 9 (**Figures 2B,C**), the ζ-potential of modified QRZ remains negative throughout the examined concentration range of HAC, likely due to the absence of free positive surface charges in the HAC structure (as seen in **Figure 2A**). Similar distributions were obtained when QRZ and HAC are dispersed in $MgSO_4$ with a slightly greater compensation of the ζ-potential of QRZ by HAC. The isoelectric point is reached in this case at approximately 0.4 $mg_{HAC}/m^2{}_{QRZ}$ in pH 5 and 0.8 $mg_{HAC}/m^2{}_{QRZ}$ in pH 7 solution. Whether the comparatively stronger change of the ζ-potential of QRZ is attributed to an enhanced adsorption of HAC or a stronger interaction with SO_4^{2-} ions compared to Cl^{-} ions cannot be unequivocally concluded at this point. However, the evolution of the ζ-potential of the mineral surface for all pH values proves that adsorption of HAC occurred and indicates the occupation of its active sites. The next stage of this work is to determine whether such differences in the ζ-potential

TABLE 2 | The used HAC concentrations in mass of HAC related to the volume of the aqueous suspension for the electrophoretic mobility tests, ACTA experiments and their equivalents displayed as mass of HAC related to the surface area of QRZ.

	Hexyl-amine cellulose nanocrystal concentration		
	Electrophoretic mobility	ACTA	Flotation
mg_{HAC}/l	$mg_{HAC}/m^2{}_{QRZ}$	$mg_{HAC}/m^2{}_{QRZ}$	$mg_{HAC}/m^2{}_{QRZ}$
0.5	0.8	–	–
1	1.6	–	–
1.5	2.4	–	–
2	3.2	–	–
2.5	4	–	–
3	4.8	0.667	0.38
5	–	1.111	0.7

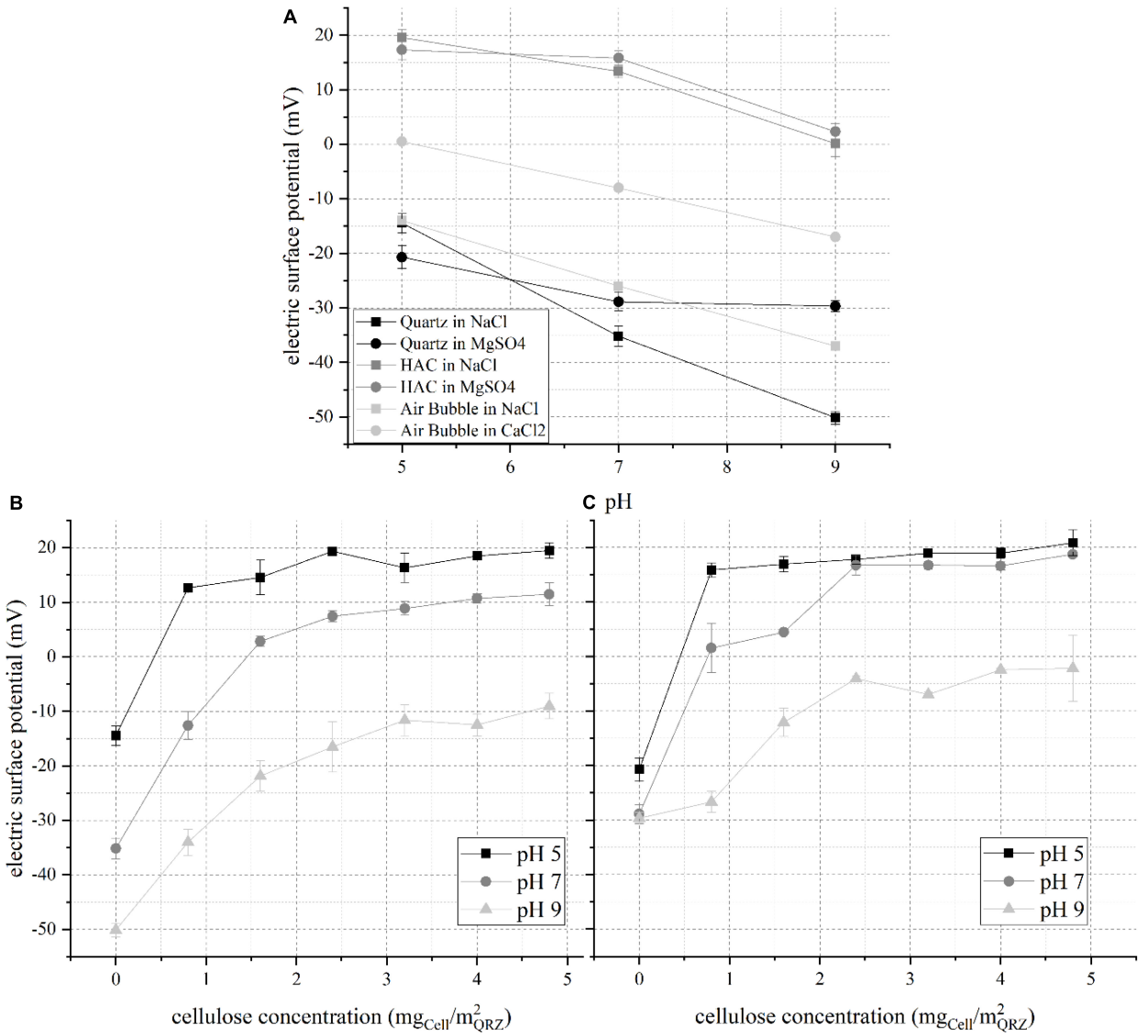

FIGURE 2 | Electric surface (ζ−) potential of **(A)** pure quartz, HAC and a bubble at different pH values according to previously published results (Yang et al., 2001; Hartmann et al., 2018), **(B)** QRZ at different HAC concentrations in NaCl, and **(C)** QRZ at different HAC concentrations in $MgSO_4$; error bars are 95% confidence intervals and lines are only visual guidelines.

are correlated to higher particle-bubble attachment probabilities and floatability.

Probability of Quartz-Bubble Attachments in the Presence of Hexyl-Amine Cellulose

As mentioned in section Materials, Methods, and Models, the probability for a QRZ particle to attach to an air bubble as a function of the particle-bubble distance (H), contact time and HAC concentration was measured by means of the ACTA. As a representative example, the results for the attachment probability are shown for pH 7 in **Figure 3**, while the results for pH 5 and pH 9 are presented in **Supplementary Figures S1, S2**.

As seen in **Figure 3**, in the absence of HAC, the bubbles had to be compressed against the particle bed (i.e., compression > 0) for attachment to occur. To obtain an attachment probability higher than 50%, bubbles were compressed for approximately 150 μm against the particle bed, which is in the range of the D_{50}-value for the QRZ particles (see **Table 1**), indicating that an attachment only occurred in the presence of an additional mechanical force acting upon the intervening liquid film rather than as a result of any attractive interfacial force. When HAC is present in solution, stable particle-bubble attachments were obtained at distances between 25 and 50 μm (P > 50%) without compressing a bubble against the particle bed (in **Figure 3**, positive distance = negative compression). In several instances, these distances exceed significantly the generally

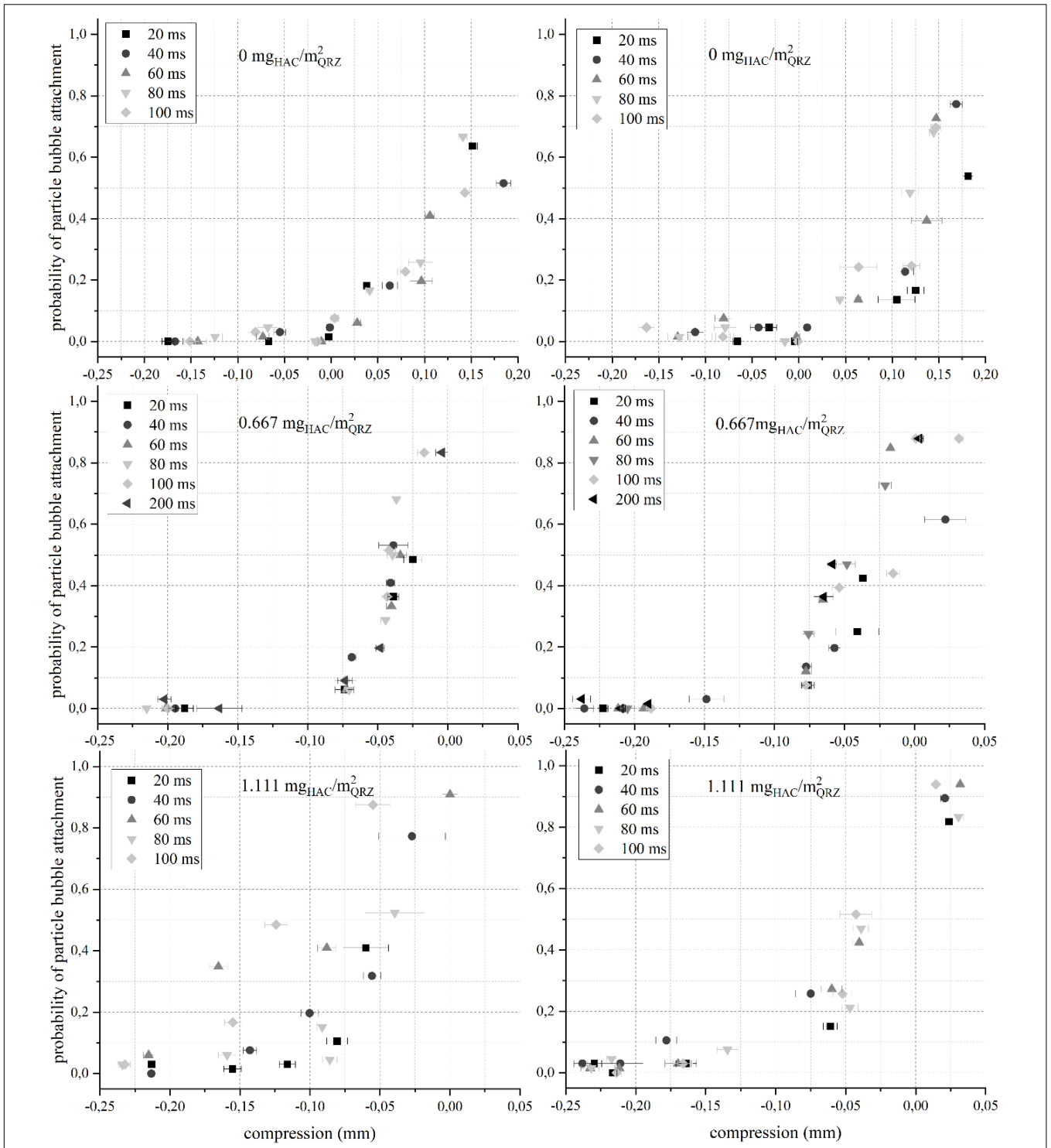

FIGURE 3 | The probability for an attachment between a QRZ particle and an air bubble immersed in a NaCl **(left)** or $MgSO_4$ **(right)** solution at pH 7 over the particle-bubble distance (compression = −H) for different contact times and HAC concentrations. The error bars are 95% confidence intervals. Note that the abscissa value range is not the same in all graphs.

accepted ranges for particle-bubble interactions (Israelachvili and Pashley, 1982; Eriksson et al., 1989; Ducker et al., 1994; Yao et al., 2016). Already when the HAC concentration was 0.667 mg$_{HAC}$/m$^2_{QRZ}$, non-compressive attachments between QRZ particles and air bubbles occurred, proving that HAC renders the mineral surface more hydrophobic, in line with earlier studies

(Laitinen et al., 2016; Hartmann et al., 2017, 2018). Interestingly, at 0.667 mg_{HAC}/m^2_{QRZ} in NaCl, the attachment probability seems rather independent from the influence of contact times, but remains sensitive to distance with a sudden increase of the attachment probability in the range between 20 and 50 μm. An additional experiment with 200 ms contact time was performed at the lower HAC concentration, however not showing a significant increase of the attachment probability in any of the background salt solutions. The independence of the attachment probability distribution in terms of the set contact time has not been reported before, but may be interpreted as a spontaneous rupture of the intervening film occurring at a significantly shorter time than the minimum contact time used in these experiments. As will be discussed next, a stronger hydrophobicity makes the influence of contact time more evident, but the emergence of a non-compressive attachment between a particle and a bubble may be already indicative of a turning point on its floatability.

As seen, when the HAC concentration was increased to 1.111 mg_{HAC}/m^2_{QRZ}, two trends were observed: (i) an extension of the particle-bubble distance at which high attachment probabilities were measured, and (ii) an evident correlation of higher attachment probabilities with increasing contact time for each given particle-bubble distance. These trends are most significant for particle-bubble attachments in NaCl solution, but were consistently seen for the attachment probabilities of QRZ for both background solutions in pH 5 or 9 (see **Supplementary Figures S1, S2**). The dependence of attachment probability to particle size was shown in a previous work to follow the efficiency of particle-bubble aggregate stability, which diminishes with increasing particle size (Hartmann and Serna-Guerrero, 2020). Admittedly, the sensitivity of attachment probabilities for different contact times in this work may be limited by the relatively broad particle size distribution, i.e., 75–180 μm. Nevertheless, non-compressive attachment has been recorded for all samples in which HAC was present and a higher sensitivity in regards of the contact time was always observed at higher HAC concentrations, demonstrating the ability of ACTA to distinguish different degrees of hydrophobicity for a particular mineral sample.

When the results are put in context with the ζ-potential of QRZ coated with HAC under identical environments, a higher adsorption capacity is expected with increasing HAC concentrations, as reflected by the compensation of the ζ-potential in **Figure 2**. Thus, at higher HAC concentrations, it can be expected that a more complete coverage of QRZ particles occurs, resulting in a higher degree of hydrophobicity. In turn, this leads to longer distances for which high attachment probabilities occur, generating an evident dependence of attachment probabilities with contact times. As shown in **Figure 2**, when the HAC concentration is 0.666 mg_{HAC}/m^2_{QRZ}, the ζ-potential of HAC-coated QRZ is more negatively charged in NaCl compared to $MgSO_4$ solution. Interestingly, the results of the particle-bubble attachment probability in $MgSO_4$ solution show a comparatively higher sensitivity in terms of contact time. By increasing the HAC concentration to 1.111 mg_{HAC}/m^2_{QRZ} at pH 7, the ζ-potential of HAC-coated QRZ approaches its iso-electric point in NaCl solution, while the potential is overcompensated in $MgSO_4$ solution. In the case of ACTA analysis, the increase of HAC concentration from 0.666 mg_{HAC}/m^2_{QRZ} to 1.111 mg_{HAC}/m^2_{QRZ} in NaCl solution led to an increase of the attachment distance and a higher sensitivity in terms of the contact time for non-compressive attachments. Surprisingly, no significant change occurred by increasing the HAC concentration in $MgSO_4$ solution, which may be explained by an antagonistic effect in terms of floatability obtained when the ζ-potential of QRZ is overcompensated by HAC, as described in an earlier work (Hartmann et al., 2018). This is an indication of the different behavior of nanocellulose compared to traditional collectors, as one may not obtain a better flotation performance simply by increasing the concentration of the former due to the random distribution of amine groups on its surface.

The obtained non-compressive particle-bubble attachments are in line with previous results obtained for the attachment of silanized glass beads to air bubbles (Hartmann and Serna-Guerrero, 2020). These results exhibit the existence of a force acting over far longer distances or perhaps changes in the properties of water molecules within the intervening liquid film have to be assumed. Although the nature of the long-range attraction cannot be analyzed in detail based on the results obtained in this work, the results of the ACTA may be a good foundation to draw some conclusions. An estimation of the length scale of micro-eddies is given after Kolmogorov (Nguyen and Schulze, 2004) by:

$$\lambda_K = \left(\frac{\nu^3}{\varepsilon}\right)^{\frac{1}{4}} \tag{2}$$

When a value for the kinematic viscosity ν of 10^{-6} m^2/s and the mean dissipation rate ε between 1 and 100 W/kg is assumed, the length of a microscale eddy is estimated between 10 and 30 μm, which is in the range of the particle-bubble distance shown in **Figure 3**. However, the results of hydrophilic QRZ particles (in the absence of HAC) show that microscale eddies do not have a significant effect on the particle-bubble attachment and particles only attach when a bubble is compressed against a particle. In other words, it is possible that microscale eddies contribute to the transportation of microparticles, but particle-bubble agglomerates result only when attractive forces are present. Admittedly, the presented values for the kinematic viscosity of vicinal water and the dissipation rate in polarized water molecules are rough estimations.

Another phenomenon that is worth considering is the ability of fluid molecules to propagate forces along their structure, which was firstly described by Hardy (1931) using the term "*diachysis*" (after the Greek *diáchysis* meaning "diffusion"). A review of experimental data suggesting the existence of an abnormal behavior of water molecules was presented 70 years ago by Henniker (1949) and some 20 years later, Padday (1970) studied the rupture of thin liquid films between surfaces with different wettability and air. In the latter work, the rupture of thin water films was detected to be initiated at thicknesses between 100 and 500 μm over surfaces with low surface energy. Although long-range forces are expected to be of structural nature (Ducker et al., 1994; Yoon and Moa, 1996),

based on an entropic effect of the re-arrangement of water molecules near hydrophobic surfaces, no conclusive physical explanation for their strength and extension has been found. One important aspect of *diachysis* is that the origin of forces is not locally restricted to the surface of particles or bubbles, but forces are acting along clusters of structured water molecules (Eriksson et al., 1989). In other words, the liquid phase is not solely a passive medium through which forces act, but it energetically merits from the presence of a solid or gaseous phase, which induce a structure into the liquid film, leading to the propagation of forces over relatively long distances. The examination of the structure of water molecules near solid or gaseous surfaces is an ongoing field of research, challenged by the complexity of the system under investigation, which at present exceeds the ability of molecular modeling (Akaishi et al., 2017). The ACTA may be a valuable technique to quantify the strength and range of interactions between microparticles and bubbles in quiescent environments. To investigate if the particle-bubble attachments occur and are stable under turbulent conditions, the flotation recovery of QRZ in the presence of HAC is presented next.

Flotation of Quartz Using Hexyl-Amine Nanocrystals

The results for the flotation of QRZ with HAC are presented in **Figure 4**, showing a significant increase of the flotation recovery between 0.38 and 0.7 mg_{HAC}/m^2_{QRZ}. The lower HAC concentration was not sufficient to render QRZ sufficiently hydrophobic and the high turbulences in the flotation cell did not contribute to produce stable three-phase contacts. For the results obtained with 0.7 mg_{HAC}/m^2_{QRZ} in NaCl solution, an increasing flotation recovery with increasing pH value was obtained, while similar recoveries were obtained at pH 7 and 9 in $MgSO_4$. The relatively high flotation recoveries obtained with 0.7 mg_{HAC}/m^2_{QRZ} also prove that, even though physisorption of HAC is assumed, it withstood its detachment from the particle surface under the action of turbulent currents in the flotation cell.

Figure 4 also compares the results of two experiments performed using HAC solution in the presence of fresh and recirculated QRZ at pH 7 and 9 in NaCl solution. While the flotation of fresh QRZ resulted in low flotation recoveries, flotation performance improved significantly after drying and re-suspension in the presence of HAC. This is understandable since, due to characteristics of the flotation setup, the amount of HAC suspension used was not excessive, which likely resulted in the reduction of the HAC bulk concentration in the suspension during physisorption of HAC on the QRZ surface. As a result, the adsorbed amount of HAC on fresh QRZ does not represent saturation at target HAC concentration. By re-dispersing QRZ in HAC suspension, the HAC adsorption approached equilibrium at the target of 5 mg/l (0.7 mg_{HAC}/m^2_{QRZ}). The same procedure was performed for the lower HAC concentration, but no increase of the floatability obtained (0.38 mg_{HAC}/m^2_{QRZ}), proving that QRZ is not rendered sufficiently hydrophobic at the low HAC concentration. An additional finding by following the aforementioned procedure is that HAC remains adsorbed throughout the process of vacuum filtration, drying and re-dispersion of the sample in the HAC solution. These observations suggest that the desorption of HAC does not occur spontaneously, at least under the conditions hereby used.

The dramatic increase of recovery from 0.38 to 0.7 mg_{HAC}/m^2_{QRZ} indicates that the change from a non-floatable to a floatable behavior takes place within a narrow window of HAC adsorption. Consequently, the flotation results obtained show that ACTA is sensible enough to detect the point at which floatability of particles become significant. Indeed, according

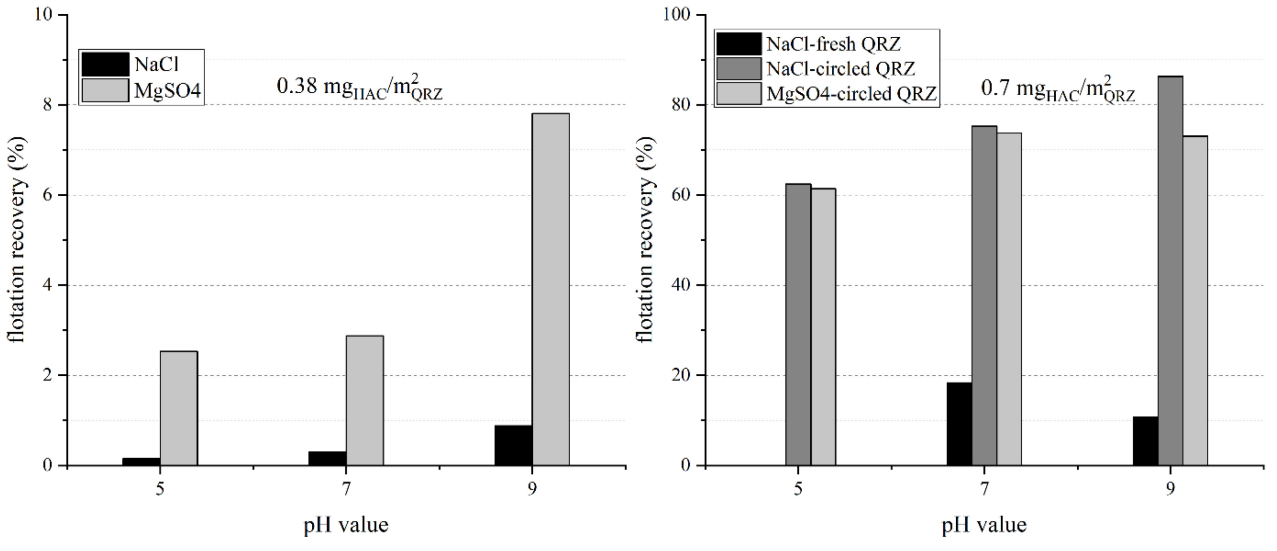

FIGURE 4 | The flotation recovery of quartz using hexyl-amine nanocrystals as collector with a concentration of 0.38 mg_{HAC}/m^2_{QRZ} **(left)** and 0.7 mg_{HAC}/m^2_{QRZ} **(right)** in different background salt solutions (shown is the mean value of two experiments).

to the ACTA results, successful non-compressive attachment is detected at 0.667 mg_{HAC}/m^2_{QRZ}. In other words, non-compressive attachments with high probability may be a suitable indicator for efficient flotation.

The correlation of the flotation results to the state of the ζ-potential of QRZ under identical conditions shows that an increasing potential does not correspond to a higher floatability. In contrast, the more negative the ζ-potential of QRZ at a HAC concentration of 0.7 mg_{HAC}/m^2_{QRZ}, the higher flotation recoveries were obtained for experiments performed in NaCl solutions. Further, the electrophoretic mobility tests indicate that at a concentration of 0.7 mg_{HAC}/m^2_{QRZ} HAC does not cover the entire QRZ surface, assuming that HAC has a tendency to form a monolayer on the QRZ surface. In accordance to the general knowledge in flotation, this shows that high flotation recoveries are also obtained for cellulose-based reagents even without the formation of an ideal monolayer on the mineral surface.

CONCLUSION

In this study, HAC was tested as an environmentally-friendly collector for the flotation of QRZ. Bench-scale flotation experiments revealed that adsorbed HAC rendered the QRZ surface more hydrophobic, leading to recoveries up to 90% at 0.7 mg_{HAC}/m^2_{QRZ}, proving that the application of cellulose-based macromolecules is feasible in turbulent froth flotation processes. The adsorption of HAC on QRZ was indicated with the help of ζ-potential measurements showing a consistent reduction of the ζ-potential of QRZ in the presence of HAC. Induction time experiments with the ACTA exhibited that high probabilities for non-compressive attachments can be obtained at distances between 25 and 50 μm in the presence of HAC, while pure QRZ only attached to air bubbles under the action of significant compression. In consequence, the ACTA and flotation results demonstrate the relevance of hydrophobic forces in the attraction between HAC-coated QRZ and air bubbles. In addition, an increase of the floatability of QRZ in a bench-scale flotation cell coincided with conditions where non-compressive particle-bubble attachments appeared in ACTA measurements. Although additional studies have to be performed to elaborate on its degree of accuracy, this work also shows the potential of the ACTA to be used for the prediction of the hydrophobicity and thus floatability of a mineral phase.

DATA AVAILABILITY STATEMENT

The datasets generated for this study are available on request to the corresponding author.

AUTHOR CONTRIBUTIONS

RH performed and overviewed the experimental work and prepared the first draft of the manuscript. RS-G reviewed the manuscript. Both had regular meetings during the experimental work and writing phase.

FUNDING

This work is part of the ACTA project supported by the Finnish Metals Producers Fund. RH would like to thank the Academy of Finland for their financial support with the "BioMInt" Postdoctoral Research project. This research benefited from the RAMI- RawMatTERS Finland Infrastructure.

ACKNOWLEDGMENTS

We would like to thank Prof. Dr. Mirja Illikainen and her group of the Fibre and Particle Engineering Research Unit at the University of Oulu for the preparation of the hexyl amine cellulose nanocrystal suspension and the opportunity to share the equipment for electrophoretic mobility measurements. Further, we would like to express their special thanks to Ms. Pia Höner for her contribution to the laboratory work.

SUPPLEMENTARY MATERIAL

The Supplementary Material for this article can be found online at: https://www.frontiersin.org/articles/10.3389/fmats.2020.00053/full#supplementary-material

FIGURE S1 | The probability for an attachment between a QRZ particle and an air bubble immersed in a NaCl or $MgSO_4$ solution at pH 5 over the particle-bubble compression for different contact times and HAC concentrations.

FIGURE S2 | The probability for an attachment between a QRZ particle and an air bubble immersed in a NaCl or $MgSO_4$ solution at pH 9 over the particle-bubble compression for different contact times and HAC concentrations.

REFERENCES

Abarca, C., Ali, M. M., and Pelton, R. H. (2018). Choosing mineral flotation collectors from large nanoparticle libraries. *J. Coll. Interf. Sci.* 2018, 423–430. doi: 10.1016/j.jcis.2018.01.080

Ago, M., Huan, S., Borghei, M., Raula, J., Kauppinen, E. I., and Rojas, O. J. (2016). High-throughput synthesis of lignin particles (∼30 nm to ∼2 μm) via aerosol flow reactor: size fractionation and utilization in pickering emulsions. *ACS Appl. Mater. Interf.* 8, 23302–23310. doi: 10.1021/acsami.6b07900

Akaishi, A., Yonemaru, T., and Nakamura, J. (2017). Formation of water layers on graphene surfaces. *ACS Omega* 2017, 2184–2190. doi: 10.1021/acsomega.7b00365

Al-Shatty, W., Lord, A. M., Alexander, S., and Barron, A. R. (2017). Tunable surface properties of aluminum oxide nanoparticles from highly hydrophobic to highly hydrophilic. *ACS Omega* 2017, 2507–2514. doi: 10.1021/acsomega.7b00279

Aspiala, M., Schreithofer, N., and Serna-Guerrero, R. (2018). Automated contact time apparatus and measurement procedure for bubble-particle interaction analysis. *Minerals Eng.* 2018, 77–82. doi: 10.1016/j.mineng.2018.02.018

Bridge, G. (2004). Contested terrain: mining and the environment. *Annu. Rev. Environ. Resour.* 29, 205–259. doi: 10.1146/annurev.energy.28.011503.163434

Calvo, G., Mudd, G., Valero, A., and Valero, A. (2016). Decreasing ore grades in global metallic mining: a theoretical issue or a global reality? *Resources* 5:36. doi: 10.3390/resources5040036

Crawford, R., and Ralston, J. (1988). The influence of particle size and contact angle in mineral flotation. *Int. J. Mineral Process.* 1988, 1–24. doi: 10.1016/0301-7516(88)90002-6

Derjaguin, B. V., and Churaev, N. V. (1989). The current state of the theory of long-range surfaec forces. *Coll. Surf.* 1989, 223–237. doi: 10.3109/10799893.2014.980950

Dong, X., Price, M., Dai, Z., Xu, M., and Pelton, R. (2017). Mineral-mineral particle collisions during flotation remove adsorbed nanoparticle flotation collectors. *J. Coll. Interf. Sci.* 2017, 178–185. doi: 10.1016/j.jcis.2017.05.050

Ducker, W. A., Xu, Z., and Israelachvili, J. N. (1994). Measurements of hydrophobic and DLVO forces in bubble-surface interactions in aqueous solutions. *Langmuir* 1994, 3279–3289.

Eriksson, J. C., Ljunggren, S., and Claesson, P. M. (1989). A phenomenological theory of long-range hydrophobic attraction forces based on a square-gradient variational approach. *J. Chem. Soc. Faraday Trans. 2* 85, 163. doi: 10.1039/f29898500163

Fuerstenau, D. W., and Jia, R. (2004). The adsorption of alkylpyridinium chlorides and their effect on the interfacial behavior of quartz. *Coll. Surf. A* 2004, 223–231. doi: 10.1016/j.colsurfa.2004.04.090

Fuerstenau, D. W., and Pradip, (2005). Zeta potentials in the flotation of oxide and silicate minerals. *Adv. Coll. Interf. Sci.* 2005, 9–26. doi: 10.1016/j.cis.2004.08.006

Hardy, W. (1931). Problems of the boundary state. *Philos. Trans. R. Soc. Lond.* 1931, 1–37.

Hartmann, R., Kinnunen, P., and Illikainen, M. (2018). Cellulose-mineral interactions based on the DLVO theory and their correlation with flotability. *Minerals Eng.* 2018, 44–52. doi: 10.1016/j.mineng.2018.03.023

Hartmann, R., Rudolph, M., Ämmälä, A., and Illikainen, M. (2017). The action of cellulose-based and conventional flotation reagents under dry and wet conditions correlating inverse gas chromatography to microflotation studies. *Minerals Eng.* 2017, 17–25. doi: 10.1016/j.mineng.2017.09.004

Hartmann, R., and Serna-Guerrero, R. (2020). Towards a quantitative analysis of the wettability of microparticles using an automated contact timer apparatus. *Minerals Eng.* 149:106240. doi: 10.1016/j.mineng.2020.106240

Hartmann, R., Sirviö, J. A., Sliz, R., Laitinen, O., Liimatainen, H., Ämmälä, A., et al. (2016). Interactions between aminated cellulose nanocrystals and quartz: adsorption and wettability studies. *Coll. Surf. A* 2016, 207–215. doi: 10.1016/j.colsurfa.2015.10.022

Henniker, J. C. (1949). The depth of the surface zone of a liquid. *Rev. Mod. Phys.* 1949, 322–341. doi: 10.1103/revmodphys.21.322

Hernandez, V. A., Ulloa, A., and Gutierrez, L. (2017). Use of wood hemicelluloses to improve copper recovery from high clay Cu-Mo ores. *Minerals Eng.* 2017, 198–200. doi: 10.1016/j.mineng.2017.06.023

Israelachvili, J. N., and Pashley, R. (1982). The hydrophobic interaction is long range, decaying exponentially with distance. *Nature* 1982, 341–342. doi: 10.1038/300341a0

Klemm, D., Heublein, B., Fink, H. P., and Bohn, A. (2005). Cellulose: fascinating biopolymer and sustainable raw material. *Angewandte Chemie* 44, 3358–3393. doi: 10.1002/anie.200460587

Laitinen, O., Hartmann, R., Sirviö, J. A., Liimatainen, H., Rudolph, M., Ämmälä, A., et al. (2016). Alkyl aminated nanocelluloses in selective flotation of aluminium oxide and quartz. *Chem. Eng. Sci.* 2016, 260–266. doi: 10.1016/j.ces.2016.01.052

Liu, W., Moran, C. J., and Vink, S. (2013). A review of the effect of water quality on flotation. *Minerals Eng.* 53, 91–100. doi: 10.1016/j.mineng.2013.07.011

Lopéz, R., Jordão, H., Hartmann, R., Ämmälä, A., and Carvalho, M. T. (2019). Study of butyl-amine nanocrystal cellulose in the flotation of complex sulphide ores. *Coll. Surf. A* 2019:123655. doi: 10.1016/j.colsurfa.2019.123655

Mu, Y., Peng, Y., and Lauten, R. A. (2016). The depression of pyrite in selective flotation by different reagent systems – A Literature review. *Minerals Eng.* 9, 143–156. doi: 10.1016/j.mineng.2016.06.018

Nguyen, A. V., and Schulze, H. J. (2004). *Colloidal Science of Flotation*. Boca Raton, FL: CRC Press.

Nuorivaara, T., Björkqvist, A., Bacher, J., and Serna-Guerrero, R. (2019). Environmental remediation of sulfidic tailings with froth flotation: reducing the consumption of additional resources by optimization of conditioning parameters and water recycling. *J. Environ. Manag.* 236, 125–133. doi: 10.1016/j.jenvman.2019.01.107

Padday, J. F. (1970). Cohesive properties of thin films of liquids adhering to a solid surface. *Specif. Discuss. Faraday Soc.* 1970, 64–74.

Pearse, M. J. (2005). An overview of the use of chemical reagents in mineral processing. *Minerals Eng.* 18, 139–149. doi: 10.1016/j.mineng.2004.09.015

Rudolph, M., and Hartmann, R. (2017). Specific surface free energy component distributions and flotabilities of mineral microparticles in flotation–An inverse gas chromatography study. *Coll. Surf. A* 2017, 380–388. doi: 10.1016/j.colsurfa.2016.10.069

Taguta, J., McFadzean, B., and O'Connor, C. (2019). The relationship between the flotation behaviour of a mineral and its surface energy properties using calorimetry. *Minerals Eng.* 2019:105954. doi: 10.1016/j.mineng.2019.105954

Taguta, J., O'Connor, C. T., and McFadzean, B. (2018). The relationship between enthalpy of immersion and flotation response. *Coll. Surf. A* 2018:263–270. doi: 10.1016/j.colsurfa.2018.08.059

van Oss, C. J. (2003). Long-range and short-range mechanisms of hydrophobic attraction and hydrophilic repulsion in specific and aspecific interactions. *J. Mol. Recogn.* 2003, 177–190. doi: 10.1002/jmr.618

Verrelli, D. I., and Albijanic, B. (2015). A comparison of methods for measuring the induction time for bubble–particle attachment. *Minerals Eng.* 2015, 8–13. doi: 10.1111/jre.12546

Visanko, M., Liimatainen, H., Sirviö, J. A., Heiskanen, J. P., Niinimäki, J., and Hormi, O. (2014). Amphiphilic cellulose nanocrystals from acid-free oxidative treatment: physicochemical characteristics and use as an oil-water stabilizer. *Biomacromolecules* 2014, 2769–2775. doi: 10.1021/bm500628g

William, A. D., Zhenghe, X., and Jacob, N. I. (1994). Measurements of hydrophobic and DLVO forces in bubble-surface interactions in aqueous solutions. *Langmuir* 1994, 3279–3289. doi: 10.1021/la00021a061

Yang, C., Dabros, T., Li, D., Czarnecki, J., and Masliyah, J. H. (2001). Measurement of the zeta potential of gas bubbles in aqueous solutions by microelectrophoresis method. *J. Coll. Interf. Sci.* 2001, 128–135. doi: 10.1006/jcis.2001.7842

Yang, S., Pelton, R., Abarca, C., Dai, Z., Montgomery, M., Xu, M., et al. (2013). Towards nanoparticle flotation collectors for pentlandite separation. *Int. J. Mineral Process.* 2013, 137–144. doi: 10.1016/j.minpro.2013.05.007

Yang, S., Pelton, R., Raegen, A., Montgomery, M., and Dalnoki-Veress, K. (2011). Nanoparticle flotation collectors: mechanisms behind a new technology. *Langmuir* 2011, 10438–10446. doi: 10.1021/la2016534

Yao, J., Han, H., Hou, Y., Gong, E., and Yin, W. (2016). A method of calculating the interaction energy between particles in minerals flotation. *Math. Probl. Eng.* 2016, 1–13. doi: 10.1155/2016/8430745

Yoon, R. H., and Moa, L. (1996). Application of Extended DLVO Theory, IV. Derivation of flotation rate equation from first principles. *J. Coll. Interf. Sci.* 181, 613–626. doi: 10.1006/jcis.1996.0419

Zembala, M. (2004). Electrokinetics of heterogeneous interfaces. *Adv. Coll. Interf. Sci.* 2004, 59–92. doi: 10.1016/j.cis.2004.08.001

Conflict of Interest: The authors declare that the research was conducted in the absence of any commercial or financial relationships that could be construed as a potential conflict of interest.